

Synoptic Meteorology I: Divergence and Vertical Motion

For Further Reading

The isobaric form of the continuity equation is presented in Section 1.3 of *Midlatitude Synoptic Meteorology* by G. Lackmann, among other references. The evaluation of divergence using integral-based methods is discussed in Section 4-4 of *Weather Analysis* by D. Djurić. The relationship between divergence and vertical motion is discussed in Section 4-5 of *Weather Analysis*. A derivation of the mass continuity equation and its basic application to vertical motion is also provided by Section 4.1 of *Mid-Latitude Atmospheric Dynamics* by J. Martin.

Why Do We Care About Vertical Motion?

We care about vertical motion for several reasons...

- Condensation, and thus cloud and precipitation formation, generally occurs from cooling an air parcel (or layer) to saturation through ascent.
- As we will demonstrate next semester, mid-latitude cyclone and anticyclone formation, decay, and movement are functions of patterns of ascent and descent.
- Vertical vorticity amplification and generation are related to vertical motion and its horizontal gradients.

One might ask, how do we evaluate vertical motion, whether qualitatively or quantitatively? In this lecture, we consider one method of doing so, by relating vertical motion to divergence. This allows us to diagnose *mechanical forcing for vertical motion* – in contrast to buoyant forcing for vertical motion, which we will discuss in the next couple of weeks.

Divergence Calculation Methods

In our previous lecture, we defined divergence as:

$$\delta = \frac{\partial u}{\partial x} + \frac{\partial v}{\partial y} \quad (1a)$$

$$\delta = \frac{\partial V}{\partial s} - V \frac{\partial \alpha}{\partial n} \quad (1b)$$

where (1a) is divergence represented in Cartesian coordinates and (1b) is divergence represented in natural coordinates. Given at least four wind observations – two each along the x - and y - or s - and n -axes – one can use centered finite difference approximations to compute divergence. This is illustrated in a Cartesian coordinate system in Fig. 1.

The process of evaluating divergence in this way can be cumbersome, however, because of the need to first convert each wind observation to its u and v components. Evaluating divergence using natural coordinates can help overcome this hurdle but is best for qualitative rather than quantitative purposes. Furthermore, because we rarely have observations over a uniform grid as in Fig. 1, we often have to interpolate data onto such a grid to calculate divergence using finite differences. Finally, recall that finite differences are approximations by their very nature and are formally valid only over finite distances (here, ∂x and ∂y). It is up to the analyst to determine whether these limitations are acceptable or not for the case being considered.

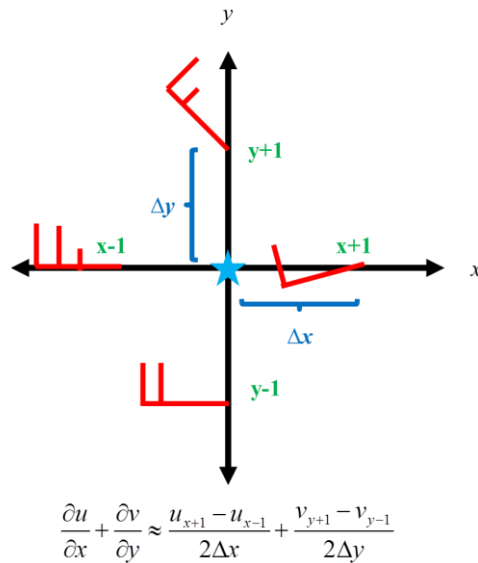


Figure 1. Conceptual example of evaluating divergence at the location given by the blue star using a centered finite difference and winds (half-flag: 5 kt, flag: 10 kt, pennant: 50 kt) from four surrounding observing locations, located at points $x-1$, $x+1$, $y-1$, and $y+1$. The distances Δx and Δy are indicated by the blue text and brackets and, formally, are in meters.

Alternatively, one could use an integral-based method to calculate the divergence into or out of any desired area. For any arbitrary two-dimensional region, the divergence within that region is defined (from calculus) as:

$$\delta = \frac{1}{A} \lim_{A \rightarrow 0} \iint_A \nabla \cdot \vec{v} da \quad (2)$$

In (2), A denotes the area of the two-dimensional region, and the double integral represents integration about the region with area A . Omitting the limit, (2) can be approximated as:

$$\delta \approx \overline{\nabla \cdot \vec{v}} = \frac{1}{A} \iint_A \nabla \cdot \vec{v} da \quad (3)$$

The overbar in (3) indicates a quantity that is averaged over the area A of the region. If we apply Green's theorem to (3), we obtain:

$$\delta = \frac{1}{A} \int_L v_n dl \quad (4)$$

In (4), L represents the boundary of the region with area A , dl represents a finite line segment along L , and v_n represents the component of the wind normal (perpendicular) to L (where $v_n > 0$ for outward-directed flow and $v_n < 0$ for inward-directed flow).

Approximating the integral in (4) with a summation, we obtain:

$$\delta \approx \frac{1}{A} \sum_{l \rightarrow L} v_n \Delta l \quad (5)$$

Equation (5) states that if we know the component of the wind normal to our region at a number of different locations along L , the distance Δl between locations along L , and the area A of the region cut out by L , we can compute the mean divergence within the region. This calculation works best when many observations – such as obtained from a model grid – are available. A conceptual example of how this may be done qualitatively is presented in Fig. 2.

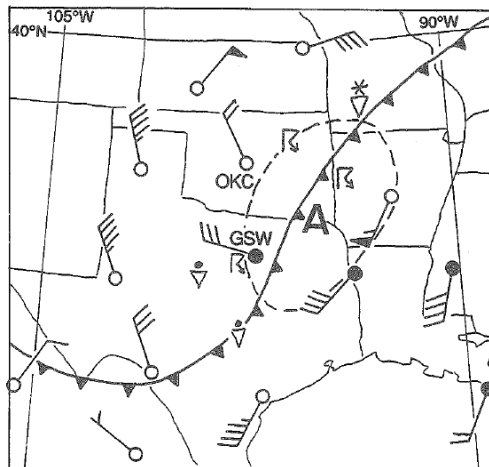


Figure 2. 850 hPa wind (barbs; half-flag: 5 kt, flag: 10 kt, pennant: 50 kt), surface frontal boundary locations (solid triangled line), and sensible weather (symbols) at 0000 UTC 27 January 1969. The dashed region surrounding location **A** is the region considered in the discussion below. Figure reproduced from *Weather Analysis* by D. Djurić, their Fig. 4-8.

Consider the portion of the dashed region located east of the surface cold front. We have two wind observations, both roughly aligned parallel to the dashed line. The normal component of the wind

at these locations, then, is zero. Given that the observations imply that the 850 hPa is out of the southwest at 40-55 kt across this entire area, there is a large inward-directed normal component of the wind on the southern edge of the dotted region. This is balanced by a large outward-directed normal component of the wind on the north-northeastern flank of the dotted region, however.

Now consider the portion of the dashed region located to the west of the surface cold front. We have two wind observations, both roughly aligned normal to the dashed line. As both are directed inward, we have a negative contribution to our summation in (5). We can infer from the wind observation in northeastern Kansas that the wind is likely roughly parallel to the dotted region on its far northern extent. Thus, summing all contributions, we assess that the mean divergence in the dotted region is negative, implying convergence. We could also explicitly calculate this using (5) by interpolating the wind observations to the dotted line, computing the normal component of the wind at each location, and determining the distance along the dotted line between each observation.

There do exist other methods of computing divergence, such as the Bellamy method for computing divergence at a location given wind observations at three nearby locations. As a result, the above is not intended to be a comprehensive listing of how divergence may be calculated. It is sufficient for our purposes, however, and enables us to move forward to relating divergence and vertical motion.

The Relationship Between Divergence and Vertical Motion

The continuity equation, expressed in isobaric coordinates, is given by:

$$\frac{\partial u}{\partial x} + \frac{\partial v}{\partial y} + \frac{\partial \omega}{\partial p} = 0 \quad (6)$$

Equation (6) states that atmospheric mass is conserved (i.e., does not change). This is clearer in the constant-height surface version of the continuity equation, which contains density ρ (with units of kg m^{-3} , or mass per unit volume), but the isobaric surface version is easier to work with. For our purposes, we will proceed as though atmospheric mass is always conserved. However, interested readers should consult Section 1.3 of *Midlatitude Synoptic Meteorology* for exceptions to this rule.

The first two terms on the left-hand side of (6) should be familiar to us by now: they represent the horizontal divergence on an isobaric surface. If we rewrite (6) with this, we obtain:

$$\delta = -\frac{\partial \omega}{\partial p} \quad (7)$$

Note that we have moved the remaining partial derivative term to the right-hand side of the equation. Equation (7) states that at a given location, the negative of the partial derivative of vertical

motion ω with respect to pressure p is equal to the divergence. Stated differently, (7) indicates that the divergence on an isobaric surface is related to how vertical velocity changes with height.

Let us now integrate (7) between two arbitrary isobaric surfaces p_b (where b refers to the bottom of the layer) and p_t (where t refers to the top of the layer), where $p_b > p_t$ (i.e., p_b is found closer to the surface than is p_t given that pressure decreases with increasing altitude). If we do so, we obtain:

$$\int_{p_b}^{p_t} \delta dp = - \int_{p_b}^{p_t} \frac{\partial \omega}{\partial p} dp \quad (8)$$

The right-hand side of (8) can be approximated as $-\int_{p_b}^{p_t} \partial \omega$, which is equal to $-(\omega(p_t) - \omega(p_b))$. If

we substitute this in to (8), we obtain:

$$\int_{p_b}^{p_t} \delta dp = -(\omega(p_t) - \omega(p_b)) \quad (9)$$

Equation (9) makes clear the relationship between divergence and vertical motion. Specifically, the difference in vertical motion ω over some vertical layer bounded by two isobaric levels p_b and p_t (where $p_b > p_t$) is equal to the vertically integrated divergence within that layer.

In this discussion, we have attributed the divergence to the divergence of the total wind. However, recall that to good approximation, we stated that the geostrophic wind is non-divergent. Thus, the divergence in this discussion can be viewed as equal to the divergence of the ageostrophic wind.

Let us now consider a hypothetical atmosphere comprised of two layers: one between the surface (p_{sfc}) and a midtropospheric isobaric level (p_L), and one between a midtropospheric isobaric level (p_L) and the tropopause (p_{trop}). This is depicted in Fig. 3 below.

Let us apply (9) for each of these two layers. For the lower layer, where $p_b = p_{sfc}$ and $p_t = p_L$, we obtain:

$$\int_{p_{sfc}}^{p_L} \delta dp = -(\omega(p_L) - \omega(p_{sfc})) \quad (10a)$$

The surface is a rigid bound on vertical motions; right at the surface, ω is equal to zero. Thus, $\omega(p_{sfc}) = 0$, such that (10a) simplifies to:

$$- \int_{p_{sfc}}^{p_L} \delta dp = \omega(p_L) \quad (10b)$$



Figure 3. Hypothetical atmosphere comprised of two layers, as described in the text above.

For the upper layer, where $p_b = p_L$ and $p_t = p_{trop}$, we obtain:

$$\int_{p_L}^{p_{trop}} \delta dp = -(\omega(p_{trop}) - \omega(p_L)) \quad (11a)$$

Due to the large atmospheric stability found at the tropopause, the tropopause itself is also treated as a rigid bound on vertical motion; at the tropopause, outside of intense small-scale ascent such as in thunderstorms, ω is equal to zero. Thus, $\omega(p_{trop}) = 0$, such that (11a) simplifies to:

$$\int_{p_L}^{p_{trop}} \delta dp = \omega(p_L) \quad (11b)$$

Upon inspection, we have two separate equations for $\omega(p_L)$, as given by (10b) and (11b). If we equate these equations, we obtain:

$$-\int_{p_{sfc}}^{p_L} \delta dp = \int_{p_L}^{p_{trop}} \delta dp \quad (12)$$

In other words, *the vertically integrated divergence in the lower layer is cancelled out by the vertically integrated divergence in the upper layer*. Stated differently, the divergence within the lower layer is equal in magnitude and opposite in sign to the divergence in the upper layer. This implies that the two are in balance with each other, such that one compensates for the other. This important principle is known as *Dines' compensation principle*.

The sign of divergence must change at least once between p_{sfc} and p_{trop} for (12) to be true. Thus, an important corollary to Dines' compensation principle states that *there must be at least one level at which the divergence is zero*. This level is the *level of non-divergence*. In the troposphere, we often find a level of non-divergence in the midtroposphere between 500-600 hPa. This is why (in part, at least) either of these standard isobaric levels are typically understood to be the *steering level* for synoptic-scale mid-latitude weather systems.

The real atmosphere typically cannot be considered by two vertical layers. However, it is relatively straightforward to evaluate the vertical profile of vertical motion given patterns of divergence even in quite complex situations. Let us start with (9), which we repeat below for simplicity:

$$\int_{p_b}^{p_t} \delta dp = -(\omega(p_t) - \omega(p_b))$$

If we let $p_b = p_{\text{sfc}}$, then $\omega(p_{\text{sfc}}) = 0$. Thus, the above equation becomes:

$$\omega(p_t) = - \int_{p_{\text{sfc}}}^{p_t} \delta dp \quad (13)$$

In other words, *the vertical motion at any isobaric level p_t is equal to the negative of the integrated divergence between the surface and p_t* ! Thus, given a vertical profile of divergence, we can start at the surface and integrate upward to obtain the corresponding vertical profile of vertical motion.

Frictionally Driven Divergence and Vertical Motion

In an earlier lecture, we noted that friction acts as a *drag* on the near-surface wind. This reduces the magnitude of the Coriolis force. Thus, whether geostrophic or gradient wind balance holds, air parcels near the surface are directed across the isobars/isohypses from high pressure/height toward low pressure/height. Consequently, *air diverges from areas of high pressure/height and converges into areas of low pressure/height near the surface*.

Because the vertically integrated divergence must be zero between the surface and the tropopause, there must be divergence above near-surface areas of low pressure/height and convergence above near-surface areas of high pressure/height. Further, there must be ascent atop near-surface areas of low pressure/height and descent atop near-surface areas of high pressure/height. This helps explain why near-surface areas of low pressure/height are often accompanied by unsettled weather (tied to ascent) and near-surface areas of high pressure/height are often accompanied by fair weather (tied to descent).

Divergence in the Four-Quadrant Jet Model

Straight/Uncurved Upper-Tropospheric Jets

Having defined divergence and diffluence in the previous lecture and linking divergence to vertical motion earlier in this lecture, we can use our newly acquired insight to obtain further information regarding jet-streak structure.

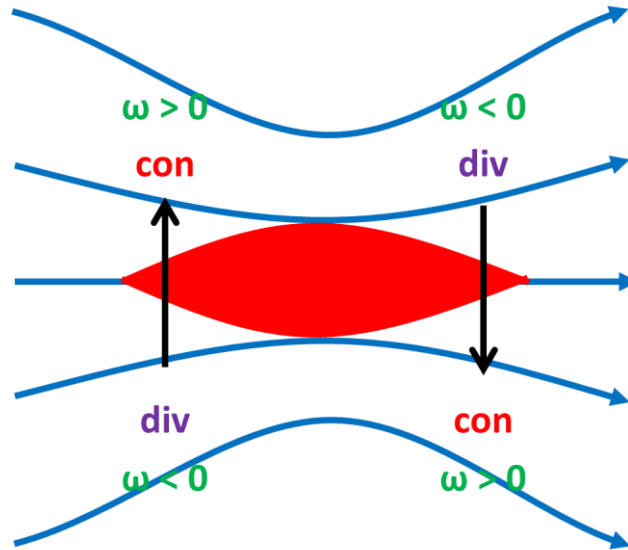


Figure 8. Idealized view of a straight westerly upper-tropospheric jet streak (in red). Hypothetical streamlines are depicted in blue, ageostrophic flow is depicted in black, the resulting convergence and divergence are depicted in red and purple respectively, and pressure vertical velocity (omega; negative values denote ascent) is depicted in green.

We first consider an idealized view of an upper-tropospheric jet streak, one that is associated with primarily “straight” flow through the jet itself. This is depicted in Fig. 8. We define a jet entrance region as the region where the wind accelerates and a jet exit region as the region where the wind decelerates. Likewise, the “right” and “left” sides of the jet are the sides of the jet with your back to the wind. For a westerly jet streak, the right side is to the south and the left side is to the north.

When we introduced the concept of the ageostrophic wind earlier this semester, we stated that it could be expressed in terms of parcel accelerations following the flow (in the absence of friction):

$$\frac{Du}{Dt} = fv_{ag} \quad (14a)$$

$$\frac{Dv}{Dt} = -fu_{ag} \quad (14b)$$

For the case of the westerly jet streak in Fig. 8, it is (14a) that we are most interested in. However, the following analysis can be generalized to a straight jet streak of any orientation.

As a parcel enters the jet, it moves from west to east at a progressively faster rate of speed, meaning that it accelerates in the eastward (or positive x -) direction. Thus, following the flow, the left-hand side of (14a) is positive as u increases. If we assume that we are in the Northern Hemisphere, such that $f > 0$, v_{ag} is positive, indicating a south-to-north flow across the jet in its entrance region. In the absence of ageostrophic flow elsewhere, this implies divergence in the right-entrance region and convergence in the left-entrance region. From Dines' compensation principle, the divergence in the right-entrance region must be balanced by lower-tropospheric convergence. From this, (13) indicates that there must be ascent in the right-entrance region maximized in the midtroposphere. Likewise, upper-tropospheric convergence in the left-entrance region must be balanced by lower-tropospheric divergence, with (13) indicating that there must be descent in the right-entrance region maximized in the midtroposphere.

Conversely, as a parcel exits the jet, it moves from west to east at a progressively slower rate of speed, meaning that it decelerates in the eastward (or positive x -) direction. Thus, following the flow, the left-hand side of (14a) is negative as u decreases. For $f > 0$, v_{ag} is negative, indicating a north-to-south flow across the jet in its exit region. In the absence of ageostrophic flow elsewhere, this implies convergence in the right-exit region and divergence in the left-exit region. Due to the same principles as in the jet entrance region, this implies midtropospheric ascent in the left-exit region and midtropospheric descent in the right-exit region.

We can take these arguments one step further. Assuming weak lower-tropospheric flow and under the constraints of the geostrophic approximation, a westerly jet streak is associated with a westerly thermal wind. A north-south layer-mean temperature gradient with cold air to the north must exist to balance this westerly thermal wind. Thus, the vertical circulation in the jet entrance region is a *direct* circulation, defined as one with ascent in the warm air and descent in the cold air, whereas the vertical circulation in the jet exit region is an *indirect* circulation, defined as one with descent in the warm air and ascent in the cold air.

Surface cyclones tend to develop, or develop most rapidly, when located in the right-entrance or left-exit regions of an upper-tropospheric jet, where ascent is indicated in Fig. 8. We will explore why this is the case in more detail next semester.

The Inclusion of Jet Curvature

Above, we considered the ageostrophic flow for a “straight” jet streak. However, jet streaks and the synoptic-scale flow accompanying them often exhibit at least weak curvature. An example of a weakly curved jet streak is depicted in Fig. 9.

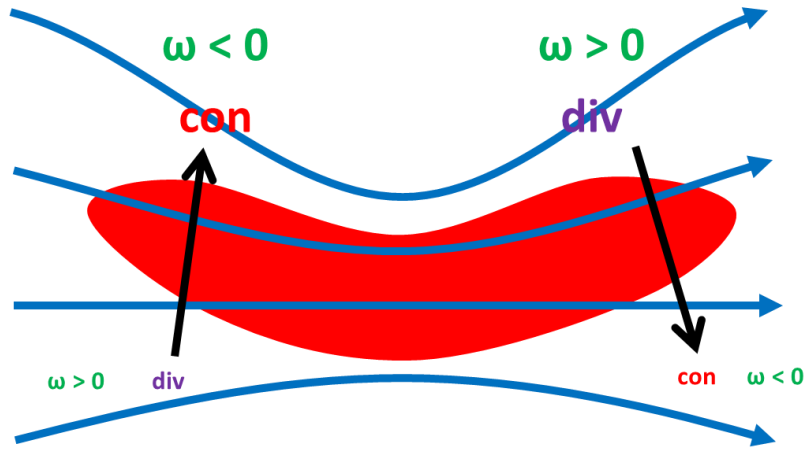


Figure 9. As in Fig. 8, except for a curved (along the streamlines) upper tropospheric jet streak. The relative size of the text on each side of the jet indicates the relative magnitudes of divergence and omega on each side of the jet.

The addition of flow curvature contributes another source of ageostrophic flow, that due to curved flow, to that associated with straight-line flow accelerations. In the example in Fig. 9, the flow has greater curvature (and thus greater ageostrophic flow) on the left side of the jet, whereas it has weaker curvature (and thus weaker ageostrophic flow) on the right side of the jet. Consequently, convergence/divergence and vertical motion are maximized on the left side of the jet in this case.

The Four-Quadrant Jet Model Applied to Lower-Tropospheric Jets

Let us consider the four-quadrant jet model applied to lower-tropospheric jets. For ease of interpretation, let us consider a southerly lower-tropospheric jet, as depicted in Fig. 10, though the basic interpretation can be applied to any lower-tropospheric jet. From (14b), the ageostrophic wind must be negative (east-to-west) in this jet's entrance region and positive (west-to-east) in this jet's exit region.

From Dines' compensation principle, lower-tropospheric convergence must be balanced by upper-tropospheric divergence, and thus (13) indicates that there must be ascent with a midtropospheric maximum in the jet regions with lower-tropospheric convergence. Likewise, lower-tropospheric divergence must be balanced by upper-tropospheric convergence, with (13) indicating that there must be descent with a midtropospheric maximum in the jet regions with lower-tropospheric divergence.

Thus, the pattern of ascent and descent is flipped from that with upper-tropospheric jets: ascent is favored in the left-entrance and right-exit regions and descent is favored in the right-entrance and left-exit regions.

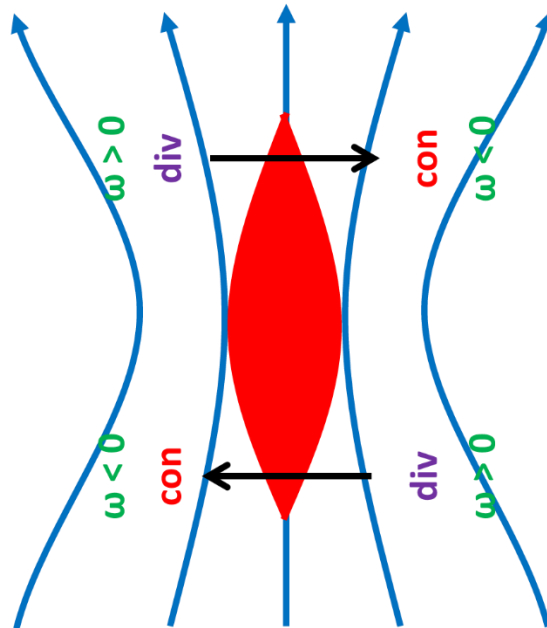


Figure 10. As in Fig. 8, except for a lower-tropospheric jet. Note that the only change between Figs. 8 and 10, apart from the direction of the jet, is the sign of omega in each quadrant.